Generalized integral representation method as applied to numerical simulation of Boussinesq wave

Gantulga Tsedendorj[1], Baljinnyam Tsangia[2], Khongorzul Dorjgotov[3,*]

[1]*Department of Mathematics, School of Arts and Sciences, National University of Mongolia, Ulaanbaatar, Mongolia*
[2]*Department of Mathematics, School of Applied Sciences, Mongolian University of Science and Technology, Ulaanbaatar, Mongolia*
[3]*Department of Applied Mathematics, School of Engineering and Applied Sciences, National University of Mongolia, Ulaanbaatar, Mongolia*
**Correspondence author. Email: khongorzul@seas.num.edu.mn*

ABSTRACT

In this study, we present discretization schemes based on Generalized Integral Representation Method (GIRM) for numerical simulation of the Boussinesq wave. The schemes numerically evaluate the coupled Boussinesq equation for different solitary wave phenomena, namely, propagation of a single soliton, head-on collision of two solitons and reflection of a soliton at a fixed wall boundary. In these three soliton interactions, we utilize different Generalized Fundamental Solutions (GFS) along with piecewise constant approximations for the unknown functions. For the case of soliton reflection at a wall, time evolution in GIRM is coupled with the Green's function in order to cope with the complicated boundary conditions that arise from the GIRM derivation. We conduct numerical experiments and obtain satisfactory approximate result for each case of the soliton interactions.

Keywords: *Numerical Simulation of Boussinesq Wave, Soliton Interactions, Generalized Integral Representation Method (GIRM), Numerical Schemes based on GIRM*

1. INTRODUCTION

Boussinesq type equations have been studied and numerically evaluated in various ways because of their importance in many computational fields particularly, in wave studies [1], [2], [3], [4]. These equations are approximations that are applicable for weakly nonlinear and dispersive long water waves of small amplitudes [5], [6]. We below briefly mention a few previous work regarding numerical study of Boussinesq equations that are most relevant to our study.

Tzirtzilakis et al. [7] applied a combination of Fourier Spectral method in space and finite differences in time to the Boussinesq equation and investigated stability properties of solitary wave propagation by varying the velocity parameter of the wave. Bratsos [8] derived a nonlinear finite difference scheme which in turn was solved by using a modified predictor-corrector scheme in order to numerically evaluate the bad and the good Boussinesq equations. Wazwaz [9] used the tanh-coth method to determinate the one-soliton solutions and a combination of Hirota's direct method to determinate the N-soliton solutions of the Boussinesq equation. Further, Dehghan and Salehi [10] employed the boundary-only mesh-free method for a numerical solution of the classical Boussinesq equation in one dimension. Walkley and Berzins [11] used unstructured triangular finite element spatial discretization coupled with an adaptive time integration for numerical solutions of two-dimensional extended Boussinesq equations. Recently, Lteif and Gerbi [12] proposed a splitting scheme for numerical simulation of higher-ordered Boussinesq waves over a flat bottom. In their second order numerical scheme, the authors have used a high-order finite volume scheme for the hyperbolic part of the governing equation and a finite difference technique for the dispersive part.

In the present study, we extend the application of Generalized Integral Representation Method (GIRM) to numerical simulation of the coupled Boussinesq equation. GIRM uses Generalized Fundamental Solution (GFS). Effects of various GFSs on GIRM were discussed in [13]. In [14], GIRM was applied to the numerical solution of two–dimensional advection–diffusion equation. Further, an unsteady diffusion problem in a circular domain was numerically investigated via GIRM in [15].

We develop numerical schemes based on GIRM and evaluate the Boussinesq equation for three different soliton interactions. Firstly, for a single-soliton (SS) case, the water bottom is considered to be flat in order to understand the behavior of propagation of a soliton as if it travels in the middle of the sea. Next, for a soliton-to-

U. Vandandoo et al. (eds.), *Proceedings of the International Conference on Applied Sciences and Engineering (ICASE 2023)*
Atlantis Highlights in Engineering 22,
https://doi.org/10.2991/978-94-6463-330-6_4

soliton (StS) case, we evaluate head-on collision of two solitons. Finally, for a soliton-to-wall (StW) case, we evaluate reflection of a soliton at vertical walls placed at the boundaries.

2. GIRM FOR BOUSSINESQ EQUATION

Let us consider water waves on a free surface of water. The flow is incompressible and irrotational in the (x, z) plane with x–horizontal and z–vertical coordinates. The water bottom is located at $z = -h$, where h is the water depth. Let $\phi(x, z, t)$ be the velocity potential and $\eta(x, t)$ be the free surface elevation. In this setting, the Boussinesq equation is given by the following set of equations:

$$\frac{\partial \eta}{\partial t} + \frac{\partial}{\partial x}\big[(\eta + h)\mathbf{v}\big] = \frac{1}{6}h^3\frac{\partial^3 \mathbf{v}}{\partial x^3} \tag{1}$$

$$\frac{\partial \mathbf{v}}{\partial t} + \mathbf{v}\frac{\partial \mathbf{v}}{\partial x} + g\frac{\partial \eta}{\partial x} = \frac{1}{2}h^2\frac{\partial^3 \mathbf{v}}{\partial t \partial x^2} \tag{2}$$

with the horizontal velocity $\mathbf{v}(x, t) = \phi(x, -h, t)$ at the bottom. Here g is the gravitational acceleration.

2.1. GIRM for SS and StS interactions

Since the Boussinesq equation expresses waves propagating to both directions of the x coordinate, we consider region $-L < x < L$, where L is large enough. We assume that the functions η and $\mathbf{v}$ (thus their derivatives) vanish at the boundary.

Firstly, we derive generic integral representations of Eqs. (1-2) for SS and StS interactions as these two cases have the same boundary conditions. Multiplying both sides of Eq. (1) by function $G = G(x, \xi)$ of variables x and ξ, and integrating it over $-L < x < L$, we obtain

$$\int_{-L}^{L}\left[\frac{\partial \eta}{\partial t} + \frac{\partial}{\partial x}\big((\eta + h)\mathbf{v}\big) - \frac{h^3}{6}\frac{\partial^3 \mathbf{v}}{\partial x^3}\right]G dx = 0. \tag{3}$$

Integrating and rearranging Eq. (3), we have

$$\begin{aligned}
&\int_{-L}^{L}\frac{\partial \eta}{\partial t}G(x, \xi)dx = \\
&-\big[(\eta + h)\mathbf{v}G\big]_{x=-L}^{x=L} + \int_{-L}^{L}(\eta + h)\mathbf{v}\frac{\partial G}{\partial x}dx \\
&+\frac{1}{6}h^3\left[\frac{\partial^2 \mathbf{v}}{\partial x^2}G\right]_{x=-L}^{x=L} - \frac{1}{6}h^3\left[\frac{\partial \mathbf{v}}{\partial x}\frac{\partial G}{\partial x}\right]_{x=-L}^{x=L} \\
&+\frac{1}{6}h^3\left[\mathbf{v}\frac{\partial^2 G}{\partial x^2}\right]_{x=-L}^{x=L} - \frac{1}{6}h^3\int_{-L}^{L}\mathbf{v}\frac{\partial^3 G}{\partial x^3}dx.
\end{aligned} \tag{4}$$

Taking into account the boundary conditions and swapping x and ξ in Eq. (4), yield us

$$\begin{aligned}
&\int_{-L}^{L}\frac{\partial \eta}{\partial t}G(\xi, x)d\xi = \\
&\int_{-L}^{L}(\eta + h)\mathbf{v}\frac{\partial G}{\partial \xi}d\xi - \frac{1}{6}h^3\int_{-L}^{L}\mathbf{v}\frac{\partial^3 G}{\partial \xi^3}d\xi,
\end{aligned} \tag{5}$$

where $G = G(\xi, x)$ is a GFS chosen properly. The determination of a GFS for GIRM is always possible in advance [13]. If η and $\mathbf{v}$ are known at time t in $-L < x < L$, then Eq. (5) is an integral equation with unknown $\partial\eta/\partial t$ in $-L < x < L$, where G is the kernel function of the integral equation.

Proceeding analogously to the above, for Eq. (2) we have

$$\int_{-L}^{L}\left[\frac{\partial \mathbf{v}}{\partial t} + \mathbf{v}\frac{\partial \mathbf{v}}{\partial x} + g\frac{\partial \eta}{\partial x} - \frac{1}{2}h^2\frac{\partial^3 \mathbf{v}}{\partial t \partial x^2}\right]G dx = 0. \tag{6}$$

Integrating and rearranging Eq. (6), we obtain

$$\begin{aligned}
&\int_{-L}^{L}\frac{\partial \mathbf{v}}{\partial t}\left[G - \frac{1}{2}h^2\frac{\partial^2 G}{\partial x^2}\right]dx = \\
&-\frac{1}{2}\left[\mathbf{v}^2 G\right]_{x=-L}^{x=L} + \frac{1}{2}\int_{-L}^{L}\mathbf{v}^2\frac{\partial G}{\partial x}dx \\
&-g\left[\eta G\right]_{x=-L}^{x=L} + g\int_{-L}^{L}\eta\frac{\partial G}{\partial x}dx \\
&+\frac{1}{2}h^2\left[\frac{\partial^2 \mathbf{v}}{\partial t \partial x}G\right]_{x=-L}^{x=L} - \frac{1}{2}h^2\left[\frac{\partial \mathbf{v}}{\partial t}\frac{\partial G}{\partial x}\right]_{x=-L}^{x=L}.
\end{aligned} \tag{7}$$

By substituting the boundary conditions and swapping x and ξ in Eq. (7), it boils down to

$$\int_{-L}^{L}\frac{\partial \mathbf{v}}{\partial t}\tilde{G}d\xi = \frac{1}{2}\int_{-L}^{L}\mathbf{v}^2\frac{\partial G}{\partial \xi}d\xi + g\int_{-L}^{L}\eta\frac{\partial G}{\partial \xi}d\xi, \tag{8}$$

with $\tilde{G} = \tilde{G}(\xi, x) = G - \frac{1}{2}h^2\frac{\partial^2 G}{\partial \xi^2}$. Again, Eq. (8) is an integral equation for $\partial\mathbf{v}/\partial t$ in $-L < x < L$, if η and $\mathbf{v}$ are given at t.

Thus, we are able to compute η and $\mathbf{v}$ numerically by using for instance, the procedure described in Algorithm 2.1.

Algorithm 1 GIRM for SS and StS cases

Initialize $\eta(x, t)$ and $\mathbf{v}(x, t)$ at given time t
for current t **do**
Compute $\frac{\partial \eta}{\partial t}$ from Eq. (5)
Compute $\frac{\partial \mathbf{v}}{\partial t}$ from Eq. (8)
Obtain η and $\mathbf{v}$ at $t + \Delta t$ via time-splitting
Increment time t by Δt
end for

For our schemes, we use a simple explicit scheme

$$\begin{aligned}
\eta(x, t + \Delta t) &= \eta(x, t) + \Delta t\frac{\partial \eta(x, t)}{\partial t} \\
\mathbf{v}(x, t + \Delta t) &= \mathbf{v}(x, t) + \Delta t\frac{\partial \mathbf{v}(x, t)}{\partial t}
\end{aligned} \tag{9}$$

in the time-splitting step. For more stable results if needed, a different time-splitting technique such as a predictor-corrector type scheme can be used.

2.2. GIRM for StW interaction

In the case of reflection of a soliton at vertical walls placed at the boundaries $x = \pm L$, boundary conditions for $\eta(x, t)$ and $\mathbf{v}(x, t)$ become respectively

$$\frac{\partial \eta(\pm L, t)}{\partial x} = 0 \text{ and } \mathbf{v}(\pm L, t) = \frac{\partial^2 \mathbf{v}(\pm L, t)}{\partial x^2} = 0.$$

By substituting these conditions into Eq. (4) and swapping x and ξ, Eq. (1) for StW case becomes

$$\int_{-L}^{L} \frac{\partial \eta}{\partial t} G(\xi, x) d\xi = \int_{-L}^{L} (\eta + h)\mathbf{v} \frac{\partial G}{\partial \xi} d\xi - \frac{1}{6}h^3 \int_{-L}^{L} \mathbf{v} \frac{\partial^3 G}{\partial \xi^3} d\xi - \frac{1}{6}h^3 \left[\frac{\partial \mathbf{v}}{\partial \xi} \frac{\partial G}{\partial \xi} \right]_{\xi=-L}^{\xi=L}. \quad (10)$$

Note that in the right-hand side of Eq. (7), terms containing the derivatives $\partial^2 \mathbf{v}/\partial t \partial x$ and $\partial \mathbf{v}/\partial t$ appear on the boundaries and this makes the computation complicated. Therefore, instead of using Eq. (7) directly, we rewrite Eq. (6) as

$$\int_{-L}^{L} \left[\frac{\partial \mathbf{v}}{\partial t} - \frac{1}{2}h^2 \frac{\partial^3 \mathbf{v}}{\partial t \partial x^2} \right] G(x, \xi) dx = -\frac{1}{2} \left[\mathbf{v}^2 G \right]_{x=-L}^{x=L} + \frac{1}{2} \int_{-L}^{L} \mathbf{v}^2 \frac{\partial G}{\partial x} dx - g \left[\eta G \right]_{x=-L}^{x=L} + g \int_{-L}^{L} \eta \frac{\partial G}{\partial x} dx. \quad (11)$$

Now taking into account the boundary conditions and swapping x and ξ in Eq. (11), Eq. (2) for StW case becomes

$$\int_{-L}^{L} \left[\frac{1}{2}h^2 \frac{\partial^2}{\partial \xi^2} \left(\frac{\partial \mathbf{v}}{\partial t} \right) - \frac{\partial \mathbf{v}}{\partial t} \right] G(\xi, x) d\xi = -\int_{-L}^{L} \left[\frac{1}{2}\mathbf{v}^2 + g\eta \right] \frac{\partial G}{\partial \xi} d\xi + g\eta(L, t)G(L, x) - g\eta(-L, t)G(-L, x). \quad (12)$$

On the other hand, Eq. (2) can be reformulated as

$$\frac{1}{2}h^2 \frac{\partial^2}{\partial x^2} \left(\frac{\partial \mathbf{v}}{\partial t} \right) - \frac{\partial \mathbf{v}}{\partial t} = f(x, t), \quad -L < x < L \quad (13)$$

with

$$f(x, t) = \mathbf{v} \frac{\partial \mathbf{v}}{\partial x} + g \frac{\partial \eta}{\partial x}. \quad (14)$$

This is a second order ordinary differential equation with respect to $\partial \mathbf{v}(x, t)/\partial t$ and $\frac{\partial \mathbf{v}(\pm L, t)}{\partial t} = 0$. It is well-known [16] that the solution of Eq. (13) is

$$\frac{\partial \mathbf{v}(x, t)}{\partial t} = \int_{-L}^{L} \Gamma(x, \xi) f(\xi, t) d\xi, \quad (15)$$

with $\frac{1}{2}h^2 \frac{\partial^2 \Gamma(x,\xi)}{\partial x^2} - \Gamma(x, \xi) = \delta(x - \xi)$ in $-L < x < L$ and $\Gamma(\pm L, \xi) = 0$, where $\delta(x)$ is the Dirac delta function. Specifically, the Green's function $\Gamma(x, \xi)$ is explicitly given by

$$\frac{h}{\sqrt{2}\sinh(\frac{2\sqrt{2}}{h}L)} \sinh(\frac{\sqrt{2}}{h}(x + L)) \sinh(\frac{\sqrt{2}}{h}(\xi - L))$$

for $-L \leqslant x \leqslant \xi$ and

$$\frac{h}{\sqrt{2}\sinh(\frac{2\sqrt{2}}{h}L)} \sinh(\frac{\sqrt{2}}{h}(\xi + L)) \sinh(\frac{\sqrt{2}}{h}(x - L))$$

for $\xi \leqslant x \leqslant L$, since $\Gamma(\xi - 0, \xi) = \Gamma(\xi + 0, \xi)$ and

$$\frac{\partial \Gamma(\xi + 0, \xi)}{\partial \xi} - \frac{\partial \Gamma(\xi - 0, \xi)}{\partial \xi} = \frac{2}{h^2}.$$

By now, we are able to compute $\eta(x, t)$ and $\mathbf{v}(x, t)$ numerically. We summarize the steps of obtaining these functions for the StW interaction in Algorithm 2.2.

Algorithm 2 GIRM for StW case

Initialize $\eta(x, t)$ and $\mathbf{v}(x, t)$ at given time t
for current t **do**
Compute $\partial \eta(x, t)/\partial t$ from Eq. (10)
Obtain $f(x, t)$ by solving Eq. (12)
Compute $\partial \mathbf{v}(x, t)/\partial t$ from Eq. (15)
Obtain η and $\mathbf{v}$ at $t + \Delta t$ by using Eq. (9)
Increment time t by Δt
end for

3. NUMERICAL SCHEMES

To carry out with numerical schemes for each case of the soliton interactions, we introduce a uniform space-time mesh as follows

$$x_i = \xi_i = -L + (i + 0.5)\Delta x, \ i = 0, 1, \ldots, N - 1,$$
$$\Delta x = \Delta \xi = 2L/N, \text{ and } t_n = n\Delta t, \ n = 0, 1, \ldots,$$

and denote

$$\eta_i^{(n)} = \eta(x_i, t_n), \mathbf{v}_i^{(n)} = \mathbf{v}(x_i, t_n),$$
$$\left[\frac{\partial \eta}{\partial t} \right]_j^{(n)} = \frac{\partial \eta(\xi_j, t_n)}{\partial t}, \left[\frac{\partial \mathbf{v}}{\partial t} \right]_j^{(n)} = \frac{\partial \mathbf{v}(\xi_j, t_n)}{\partial t}, \text{etc.}$$

3.1. Numerical schemes for SS and StS cases

For the SS and StS interactions, we prepare the following approximations for discretizating Eq. (5)

$$\int_{-L}^{L} \frac{\partial \eta}{\partial t} G(\xi, x) d\xi = \sum_{j=0}^{N-1} \int_{\xi_j^-}^{\xi_j^+} \frac{\partial \eta(\xi, t_n)}{\partial t} G(\xi, x) d\xi = \sum_{j=0}^{N-1} \Lambda_j(x) \left[\frac{\partial \eta}{\partial t} \right]_j^{(n)}, \quad (16)$$

$$\int_{-L}^{L} (\eta + h)\mathbf{v} \frac{\partial G(\xi, x)}{\partial \xi} d\xi = \sum_{j=0}^{N-1} \int_{\xi_j^-}^{\xi_j^+} (\eta(\xi, t_n) + h)\mathbf{v}(\xi, t_n) \frac{\partial G}{\partial \xi} d\xi = \sum_{j=0}^{N-1} \Theta_j(x)\mathbf{v}_j^{(n)}(\eta_j^{(n)} + h), \quad (17)$$

$$\int_{-L}^{L} \mathbf{v} \frac{\partial^3 G(\xi, x)}{\partial \xi^3} d\xi = \sum_{j=0}^{N-1} \int_{\xi_j^-}^{\xi_j^+} \mathbf{v}(\xi, t_n) \frac{\partial^3 G}{\partial \xi^3} d\xi = \sum_{j=0}^{N-1} \Phi_j(x)\mathbf{v}_j^{(n)}, \quad (18)$$

and the following approximations for Eq. (8)

$$\int_{-L}^{L} \frac{\partial \mathbf{v}}{\partial t}\tilde{G}(\xi,x)d\xi = \sum_{j=0}^{N-1}\int_{\xi_j^-}^{\xi_j^+} \frac{\partial \mathbf{v}(\xi,t_n)}{\partial t}\tilde{G}d\xi = \sum_{j=0}^{N-1}\Psi_j(x)\left[\frac{\partial \mathbf{v}}{\partial t}\right]_j^{(n)}, \tag{19}$$

$$\int_{-L}^{L} \mathbf{v}^2\frac{\partial G(\xi,x)}{\partial \xi}d\xi = \sum_{j=0}^{N-1}\int_{\xi_j^-}^{\xi_j^+} \mathbf{v}^2(\xi,t_n)\frac{\partial G}{\partial \xi}d\xi = \sum_{j=0}^{N-1}\Theta_j(x)\left[\mathbf{v}_j^{(n)}\right]^2, \tag{20}$$

$$\int_{-L}^{L} \eta\frac{\partial G(\xi,x)}{\partial \xi}d\xi = \sum_{j=0}^{N-1}\int_{\xi_j^-}^{\xi_j^+} \eta(\xi,t_n)\frac{\partial G}{\partial \xi}d\xi = \sum_{j=0}^{N-1}\Theta_j(x)\eta_j^{(n)}, \tag{21}$$

respectively, with

$$\Lambda_j(x) = \int_{\xi_j^-}^{\xi_j^+} G(\xi,x)d\xi,$$
$$\Psi_j(x) = \int_{\xi_j^-}^{\xi_j^+} \tilde{G}(\xi,x)d\xi,$$
$$\Theta_j(x) = \int_{\xi_j^-}^{\xi_j^+} \frac{\partial G(\xi,x)}{\partial \xi}d\xi,$$
$$\Phi_j(x) = \int_{\xi_j^-}^{\xi_j^+} \frac{\partial^3 G(\xi,x)}{\partial \xi^3}d\xi,$$

where $\xi_j^- = \xi_j - \Delta\xi/2$ and $\xi_j^+ = \xi_j + \Delta\xi/2$.
Now by utilizing the above piecewise constant approximations for the unknown functions i.e. Eqs. (16-21), Eq. (5) and Eq. (8) can be discretized resp. as

$$\sum_{j=0}^{N-1}\Lambda_j(x)\left[\frac{\partial \eta}{\partial t}\right]_j^{(n)} = \sum_{j=0}^{N-1}\Theta_j(x)\mathbf{v}_j^{(n)}(\eta_j^{(n)}+h) - \frac{1}{6}h^3\sum_{j=0}^{N-1}\Phi_j(x)\mathbf{v}_j^{(n)}, \tag{22}$$

$$\sum_{j=0}^{N-1}\Psi_j(x)\left[\frac{\partial \mathbf{v}}{\partial t}\right]_j^{(n)} = \sum_{j=0}^{N-1}\Theta_j(x)\left(g\eta_j^{(n)} + \frac{1}{2}\left[\mathbf{v}_j^{(n)}\right]^2\right). \tag{23}$$

The unknowns in Eq. (22) and Eq. (23) are the time derivatives $\left[\frac{\partial \eta}{\partial t}\right]_j^{(n)}$ and $\left[\frac{\partial \mathbf{v}}{\partial t}\right]_j^{(n)}$ respectively, and these equations are satisfied at the interior points of the mesh: $x_0, x_1, \ldots, x_{N-1}$. Hence, we have two simultaneous linear systems each of which is of N equations for N unknowns.

3.2. Numerical scheme for StW case

In this case, from Eq. (10) we have the following discretized equation for $\partial\eta/\partial t$

$$\sum_{j=0}^{N-1}\Lambda_j(x)\left[\frac{\partial \eta}{\partial t}\right]_j^{(n)} = \sum_{j=0}^{N-1}\Theta_j(x)\mathbf{v}_j^{(n)}(\eta_j^{(n)}+h) - \frac{h^3}{6}\sum_{j=0}^{N-1}\Phi_j(x)\mathbf{v}_j^{(n)} - \frac{h^3}{6}\left[\frac{\partial \mathbf{v}(L,t_n)}{\partial \xi}\frac{\partial G(L,x)}{\partial \xi} - \frac{\partial \mathbf{v}(-L,t_n)}{\partial \xi}\frac{\partial G(-L,x)}{\partial \xi}\right]. \tag{24}$$

Using Eq. (15) together with Eq. (12), we have the following equation for $\partial\mathbf{v}/\partial t$

$$\left[\frac{\partial \mathbf{v}}{\partial t}\right]_j^{(n)} = \sum_{j=0}^{N-1}\hat{\Gamma}_j(x)f_j^{(n)} \tag{25}$$

with

$$f_j^{(n)} = -\sum_{j=0}^{N-1}\Theta_j(x)\left(\frac{1}{2}\left(\mathbf{v}_j^{(n)}\right)^2 + g\eta_j^{(n)}\right) + g\eta(L,t_n)G(L,x) - g\eta(-L,t_n)G(-L,x), \tag{26}$$

where $\hat{\Gamma}_j(x) = \int_{\xi_j^-}^{\xi_j^+}\Gamma(x,\xi)d\xi$, $j = 0,1,...,N-1$. Again, Eq. (24) is a linear system of N equations for N unknowns $[\partial\eta/\partial t]_j^{(n)}$, if we use for instance, the following finite differences

$$\frac{\partial \mathbf{v}(-L,t_n)}{\partial \xi} = \frac{2}{\Delta\xi}\left[\mathbf{v}(x_0,t_n) - \mathbf{v}(-L,t_n)\right]$$
$$\frac{\partial \mathbf{v}(L,t_n)}{\partial \xi} = \frac{2}{\Delta\xi}\left[\mathbf{v}(L,t_n) - \mathbf{v}(x_{N-1},t_n)\right].$$

Finally, Eq. (25) is a linear system of N equations for N unknowns $[\partial\mathbf{v}/\partial t]_j^{(n)}$ along with Eq. (26).

4. NUMERICAL EXPERIMENTS

4.1. Numerical results of SS and StS cases

Numerical experiments for these two cases are conducted straightforward by using Eq. (22) and Eq. (23). The initial conditions are taken as $\mathbf{v}(x,0) = 0$ and

$$\eta(x,0) = \eta_0\text{sech}^2(\sigma x) \tag{27}$$

for the SS case and

$$\eta(x,0) = \eta_0\left[\text{sech}^2(\sigma(x-\tfrac{L}{5})) + \text{sech}^2(\sigma(x+\tfrac{L}{5}))\right] \tag{28}$$

for the StS case, respectively. Here $\sigma = \sqrt{3\eta_0/4h^3}$. In each of these cases, we use common Gaussian GFS

$$G(x,\xi) = \frac{1}{\sqrt{2\pi}\gamma}\exp\left(-\frac{(x-\xi)^2}{2\gamma^2}\right) \tag{29}$$

and same parameter values for comparison of the solution behaviors. Values for the parameters used in the experiments are given in Table 1 (middle column). Numerical results are shown in Fig. 1 and Fig. 2.

Table 1. Values of the simulation parameters

Parameters descriptions	Values used for	
	SS, StS cases	*StW case*
Initial depth of water h	1.0	1.0
Initial amplitude η_0	0.1	0.2
Comput. region $[-L, L]$	[-64,64]	[-50,50]
No. of division N	320	500
Mesh step Δx	0.4	0.2
Time step Δt	0.005	0.0025
Scale of GFS γ	0.3	0.15

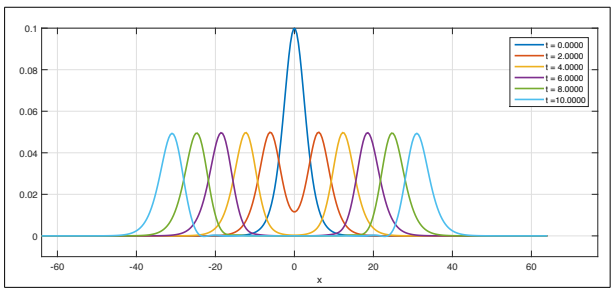

Figure 1 Simulation plot of SS case.

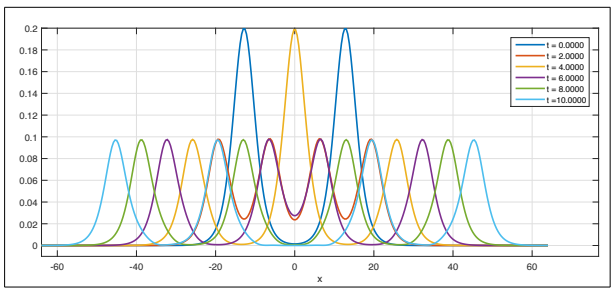

Figure 2 Simulation plot of StS case.

4.2. Numerical results of StW case

Using the Gaussian GFS given by Eq. (29) for a non-zero boundary value problem produces unsatisfactory numerical results [13]. In the StW case, it causes spurious oscillations in the solution as soon as the soliton interacts with the wall (see Fig. (3)). Therefore, in this case we take the harmonic GFS

$$G(x,\xi) = \frac{1}{2}|x-\xi|$$

and treat the derivatives of $G(x,\xi)$ as

$$\frac{\partial^2 G}{\partial x^2} = \delta(x-\xi) \text{ and } \frac{\partial^3 G}{\partial x^3} = \frac{\partial \delta(x-\xi)}{\partial x}$$

through the following properties of the delta function

$$\int \frac{\partial^2 G}{\partial x^2} f(\xi) d\xi = f(x) \text{ and } \int \frac{\partial^3 G}{\partial x^3} f(\xi) d\xi = \frac{df(x)}{dx}.$$

Numerical experiments are conducted by using Eqs. (24-26). The initial conditions are given by Eq. (27) and values for the parameters used in the experiments are given in Table 1 (last column). The numerical result of the StW case with the harmonic GFS is shown in Fig. (4). For comparison purpose, we also evaluate the StW interaction by using Finite Difference Method (FDM) coupled with the Green's function and provide the solution plot in Fig. (5). It can be seen that the former solution plot in Fig. (4) is more accurate than the latter one in Fig. (5).

For further numerical demonstration, we compute a combination of the StS and StW interactions or shortly soliton-to-soliton-to-wall (StStW) interaction with the harmonic GFS. In this experiment, we take the initial condition given by Eq. (28) and the same parameter values that were used in the StW experiments. The solution plot is shown on the top of Fig. (6). The numerical result is accurate and interesting. For the purpose of visual convenience, we show this result at several chosen timesteps on the bottom part of Fig. (6).

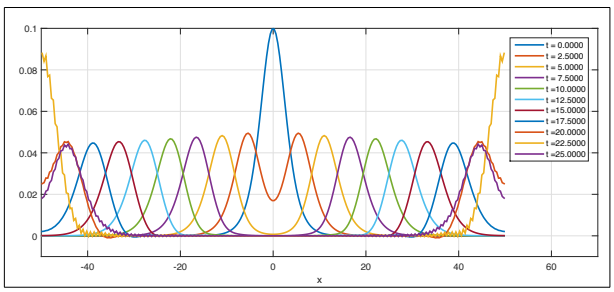

Figure 3 Solution plot of StW case obtained by GIRM with the Gaussian GFS.

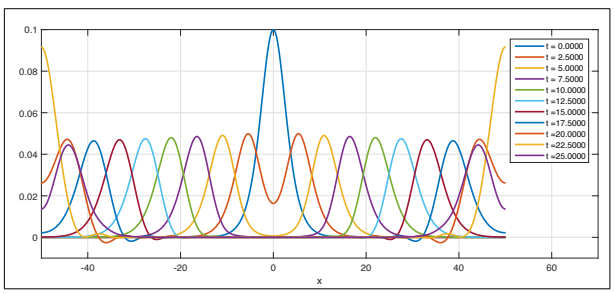

Figure 4 Solution plot of StW case obtained by GIRM with the harmonic GFS.

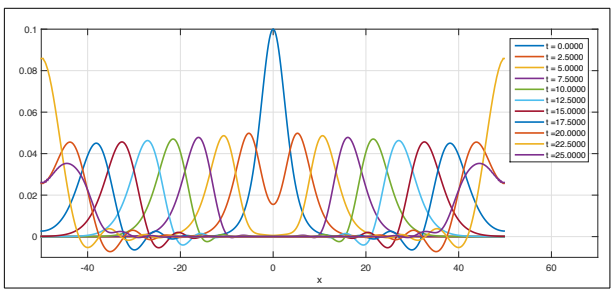

Figure 5 Solution plot of StW case obtained by FDM.

5. CONCLUSION

In this study, we develop numerical schemes based on GIRM for the coupled Boussinesq equation for simulating propagation of a single soliton, soliton-to-soliton and soliton-to-wall interactions. We emphasize the last case where GIRM is coupled with the Green's function in order to evaluate reflection of a soliton at a vertical wall. In this way we avoid computing complicated partial derivatives that appear on the boundary. This idea of treating time evolution in GIRM through the Green's function can also be applied to other numerical techniques such as FDM. For further numerical demonstration, a combination of soliton-to-soliton and soliton-to-wall interactions is also included. For each wave interaction above, we conduct numerical experiment and obtain satisfactory result.

By their constructions, our schemes do not require continuity of the approximate solutions across the mesh intervals. We use piecewise constant approximations for the unknown functions (with different GFSs) and thus it is appropriate for coarse meshes. The schemes are simple and it is easy–to–program.

ACKNOWLEDGEMENTS

The first author would like to thank the School of Arts and Sciences, National University of Mongolia for their partial support. This work was supported by the Mongolian Foundation for Science and Technology (Grant No. SHUTBIKHKHZG-2022/164).

REFERENCES

[1] P.A. Madsen, and H.A. Schaffer, A Review of Boussinesq-type Equations for Surface Gravity Waves, Advances in Coastal and Ocean Engineering, Philip L-F Liu. World Scientific, 5 (1999), pp. 1–94. https://doi.org/10.1142/9789812797544_0001

[2] J.L. Bona, M. Chen, and J.-C. Saut, Boussinesq equations and other systems for small–amplitude long waves in nonlinear dispersive media: II. The nonlinear theory, Nonlinearity, 17-3 (2004) pp. 925–952, IOP Publishing. https://doi.org/10.1088/0951-7715/17/3/010

[3] J.L. Bona, T. Colin, and D. Lannes, Long wave approximations for water waves, Arch. Rational Mech. Anal., 178 (2005), pp. 373–410. https://doi.org/10.1007/s00205-005-0378-1

[4] N.D. Katopodes, Free Surface Flow: Environmental Fluid Mechanics, 1st edition, Butterworth-Heinemann, 2018.

[5] R.S. Johnson, A modern introduction to the mathematical theory of water waves, Cambridge Texts in Applied Mathematics. Cambridge University Press, Cambridge, 1997.

[6] M.D. Todorov,'Nonlinear Waves - Theory, computer simulation, experiment, Morgan & Claypool Publishers, 2018. https://doi.org/10.1088/978-1-64327-047-0

[7] E.E. Tzirtzilakis, Ch. Skokos and T.C. Bountis, Numerical solution of the Boussinesq equation using spectral methods and stability of solitary wave propagation, First International Conference From Scientific Computing to Computational Engineering, (1st IC-SCCE), Athens, Greece, 8–10, September 2004.

[8] A.G. Bratsos, A second order numerical scheme for the solution of the one–dimensional Boussinesq equation, Numerical Algorithms, 46-1 (2007), pp. 45–58, 2007. https://doi.org/10.1007/s11075-007-9126-y

[9] A.M. Wazwaz, Multiple-soliton solutions for the Boussinesq equation, Applied Mathematics and Computation, 192-2 (2007), pp. 479–486. https://doi.org/10.1016/j.amc.2007.03.023

[10] M. Dehghan, and R. Salehi, A meshless based numerical technique for travelling solitary wave solution of Boussinesq equation, Applied Mathematical Modelling, 36-5 (2012), pp. 1939–1956. https://doi.org/10.1016/j.apm.2011.07.075

[11] M. Walkley, and M. Berzins, A finite element method for the two-dimensional extended Boussinesq equations, International Journal for Numerical Methods in Fluids, 39-10 (2002), pp. 865-885. https://doi.org/10.1002/fld.349

[12] R. Lteif, and S. Gerbi, A new class of higher-ordered/extended Boussinesq system for efficient numerical simulations by splitting operators, Applied Mathematics and Computation, 432, 127373, November 2022. https://doi.org/10.1016/j.amc.2022.127373

[13] H. Isshiki, Effects of Generalized Fundamental Solution on Generalized Integral Representation Method, Appl. Comput. Math., Special issue 4, no. 3–1 (2015), pp. 40–51. https://doi.org/10.11648/j.acm.s.2015040301.13

[14] G. Tsedendorj, and H. Isshiki, Numerical solution of two-dimensional advection–diffusion equation using generalized integral representation method, Int. J. Comput. Methods., 14:1750028 (2017), pp. 1–13. https://doi.org/10.1142/S0219876217500281

[15] G. Tsedendorj, and H. Isshiki, Numerical study of unsteady diffusion in circle, Comp. Appl. Math., 38, 26 (2019). https://doi.org/10.1007/s40314-019-0794-8

[16] D. Skinner, Mathematical Methods, Lecture notes, Chapters 6–7, University of Cambridge, pp. 74–95. https://www.damtp.cam.ac.uk/user/dbs26/

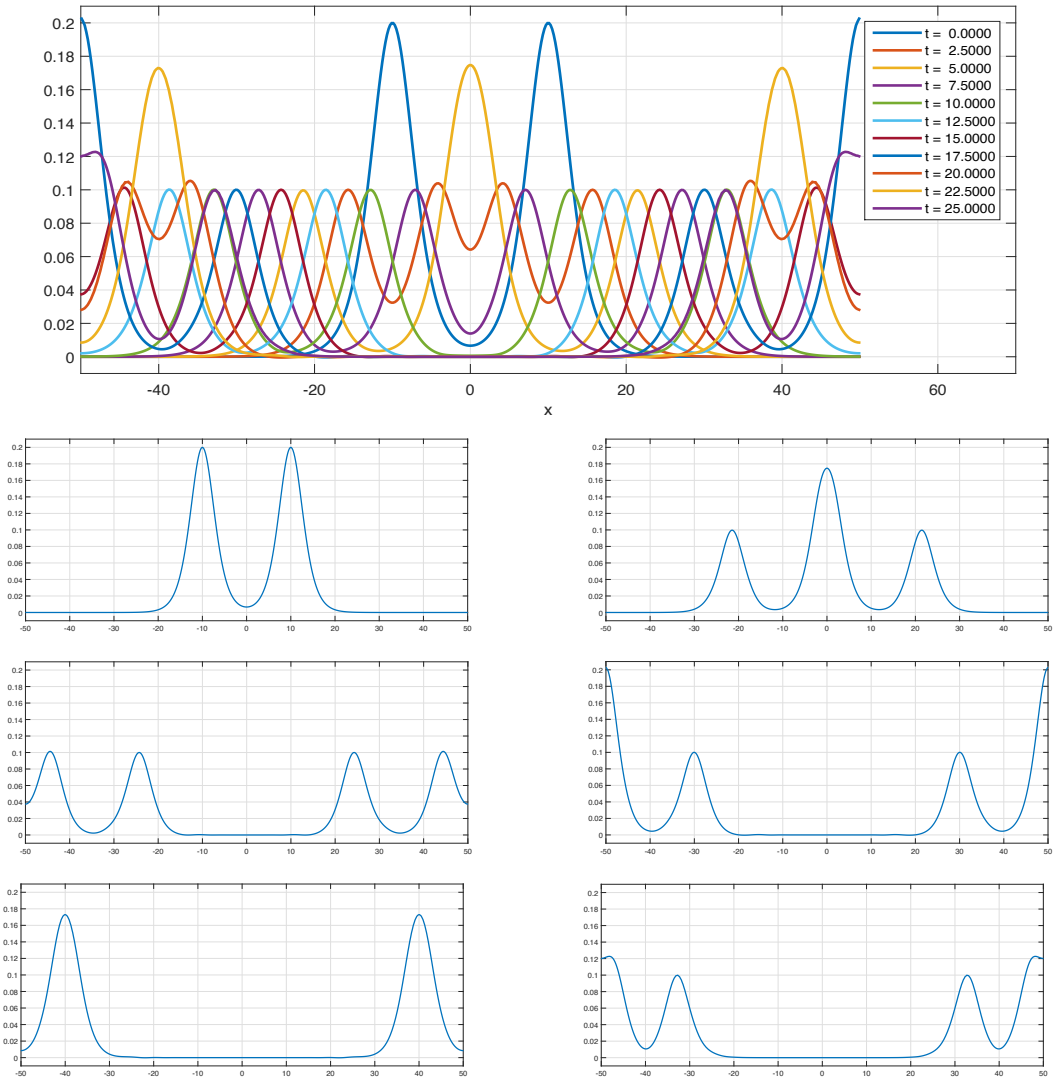

Figure 6 Solution plot of StStW interaction obtained by GIRM with the harmonic GFS (top figure). This plot is shown below in time–by–time manner at timesteps $t = 0.0; 5.0; 15.0; 17.5; 22.5; 25.0$ (from left top to right down).